Modeling Zeolites with Metal-Supported Two-Dimensional Aluminosilicate Films**

Jorge Anibal Boscoboinik, Xin Yu, Bing Yang, Frank Daniel Fischer, Radosław Włodarczyk, Marek Sierka, Shamil Shaikhutdinov, Joachim Sauer,* and Hans-Joachim Freund*

Zeolites are one of the most widely used materials in heterogeneous catalysis. However, the current understanding of the relation between structure and reactivity of these complex and highly porous materials mostly comes from studies employing bulk-sensitive techniques and from theoretical calculations based on educated assumptions about the inner surface within the pores present in the framework.[1] Zeolite frameworks are formed by ordered arrangements of $[SiO_{4/2}]$ and $[AlO_{4/2}^-]$ tetrahedra, conferring the characteristic negative charge to the system, which is typically compensated by extra-framework metal cations M^{n+} or H^+. Modeling such materials under controlled conditions, and taking advantage of the analytical tools commonly used in surface science, would provide a new playground for exploring structures and chemical reactions on zeolites. The preparation of well-defined aluminosilicate thin films was first reported using a Mo(112) substrate.[2] It was shown that this film consists of a single layer network of corner-sharing $[SiO_{4/2}]$ tetrahedra and $[AlO_{3/2}]$ units, and the film is strongly bound to the Mo(112) surface by Si-O-Mo linkages (Figure 1 a). Certainly, for those monolayer films the metal support has to be explicitly included in the proper description of the system. Furthermore, this film lacks the negative framework charge present in zeolites, which is responsible for the presence of acidic OH groups. To create a more adequate model system, herein we present the preparation of aluminosilicate films that a) are constituted of tetrahedral $[SiO_4]$ and $[AlO_4^-]$ building blocks, b) are weakly bound to the underlying metal support, and c) expose highly acidic OH species. Our results open up an avenue for experimental and theoretical modeling of zeolite surfaces that is aimed at a fundamental understanding of structure–reactivity relationships in those materials.

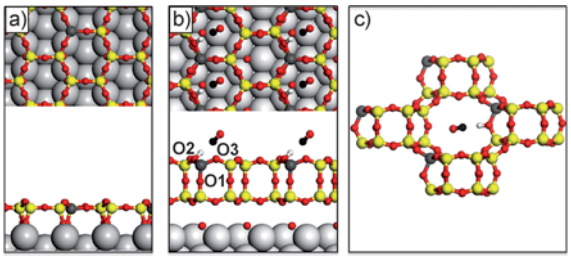

Figure 1. Structural models of a) an $AlSi_7O_{19}$ film on Mo(112); b) a $HAlSi_7O_{16}$ film on O(2×1)/Ru(0001); and c) chabasite (H-CHA) with the proton on O1. Top and cross views are shown in (a) and (b), adsorbed CO are shown in (b) and (c). One of the surface O atoms on Ru(0001) underneath the film is not seen in the top view. Si yellow, O red, Al dark gray, C black, H white.

As a starting point for the preparation of the aluminosilicate films, we used the recently reported preparation of a silica bilayer film weakly bound to a metal, in this case, Ru(0001) (see Figure 1 b).[3] The structure allows oxygen atoms to reversibly adsorb directly on the metal surface underneath the silica film,[4] which can be grown either in the crystalline or vitreous state.[3,5,6] We will refer to all these films as silica films. For aluminosilicate films, reported here (see Experimental Section), the sum of the molar amounts of Si and Al was equal to the amounts of Si necessary to prepare the bilayer silica film. The structural characterization was performed by X-ray photoelectron spectroscopy (XPS), scanning tunneling microscopy (STM), and infrared reflection–absorption spectroscopy (IRAS), in combination with density functional theory (DFT) calculations.

Using a silica film as a reference sample, the XPS results show that both Si and Al are in the highest oxidation states. For the O 1s core level, a signal at about 530.7 eV develops as a shoulder to the main peak at 531.7 eV that originates from the O atoms surrounded solely by Si in the silica films (Supporting Information, Figure S1). This shoulder becomes more prominent at increasing Al/Si ratios and it has previously been assigned to the Al-O-Si linkage.[2] The fact that the integral O 1s signal intensity remains practically constant upon Al doping is consistent with Al substituting Si in the $[SiO_4]$ tetrahedra, giving an $Al_xSi_{(1-x)}O_2$ composition, where x is the Al molar fraction.

At low Al/Si ratios, the resulting aluminosilicate surfaces show only (2 × 2) LEED patterns and are nearly atomically flat. STM images of an $Al_{0.12}Si_{0.88}O_2$ film, revealed irregularly shaped areas (marked A in Figure 2) with a slightly different

[*] Dr. J. A. Boscoboinik, X. Yu, Dr. B. Yang, Dr. S. Shaikhutdinov, Prof. Dr. H.-J. Freund
Fritz Haber Institute of the Max Planck Society
Chemical Physics Department
Faradayweg 4-6, 14195 Berlin (Germany)
E-mail: shaikhutdinov@fhi-berlin.mpg.de
F. D. Fischer, R. Włodarczyk, Prof. Dr. J. Sauer
Humboldt-Universität zu Berlin, Department of Chemistry
Unter den Linden 6, 10009 Berlin (Germany)
E-mail: js@chemie.hu-berlin.de
Prof. Dr. M. Sierka
Friedrich-Schiller-Universität Jena
Institute of Materials Science and Technology
Löbdergraben 32, 07743 Jena (Germany)

[**] This work has been supported by the German Science Foundation (DFG). J.A.B. gratefully acknowledges a fellowship by the Alexander von Humboldt Foundation.

Supporting information for this article is available on the WWW under http://dx.doi.org/10.1002/anie.201201319.

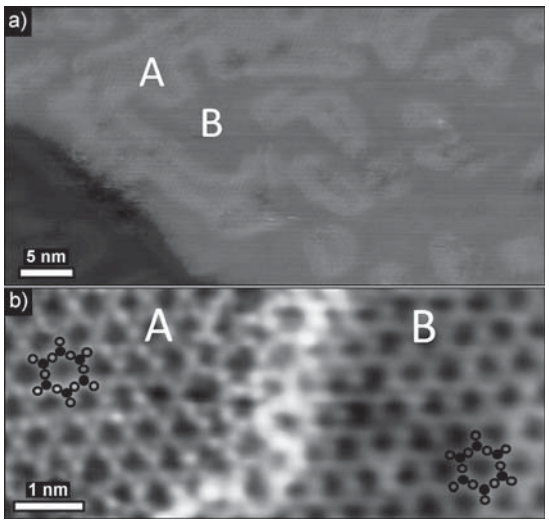

Figure 2. a) Large-scale STM image of an $Al_{0.12}Si_{0.88}O_2$ film. b) High-resolution STM image showing different contrast inside the islands A. The positions of the Si atoms in the top layer are shown by black circles and O atoms by open circles. Tunneling parameters: bias 0.15 V, current 0.07 nA.

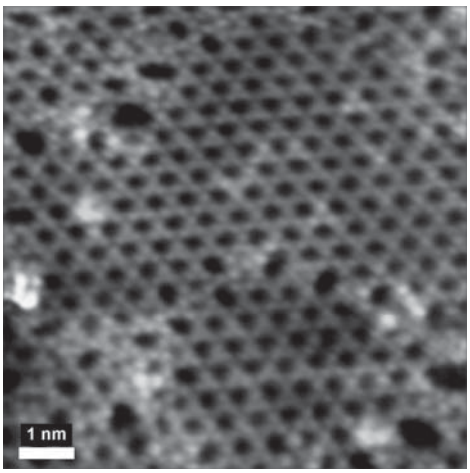

Figure 3. STM image of the $Al_{0.36}Si_{0.64}O_2$ film. Most of the surface shows the same honeycomb-like structure as observed for low Al contents, while some regions of the surface show disordered regions with rings of different sizes such as in vitreous silica. Tunneling parameters: bias 1.05 V, current 0.09 nA.

contrast, separated by protruding domain boundaries. Outside these domains, the STM images are typical of the ordered silica films,[3,6] showing the honeycomb-like structure with a rather uniform atomic contrast (marked B). Inside of domains A, the protrusions assigned to the positions of the oxygen atoms in the topmost layer are much more pronounced. The surface area covered by these domains increases with the amount of aluminum. The results therefore suggest that the Al atoms are not randomly distributed across the surface, but segregate into domains. This finding is not trivial, since it contradicts Dempsey's statement,[7] based on electrostatic considerations, that Al atoms arrange in zeolitic structures as far as possible from each other. In contrast, the strain induced by defects (an Al atom can be seen as a defect) is often minimized when the defects are located near each other. As a result of this delicate balance, Al-O-Si-O-Al linkages can be favorable under certain conditions, in particular within four-membered silica rings,[8] which are also present in our silica films, where they connect the top and bottom layers of six-membered rings.

The films preserve a flat morphology upon further increasing the Al content (Supporting Information, Figure S2), indicating that Al incorporates into the silica framework rather than forming an alumina phase. The surface is rather uniform and exposes both ordered and disordered structures, as shown on Figure 3 for the $Al_{0.36}Si_{0.64}O_2$ film. The disordered areas resemble the structure of the two-dimensional vitreous silica with a variety of *n*-membered rings.[5] For films with an Al molar fraction approaching 0.5 (that is, Al/Si = 1), the integrity of the film is not conserved, as judged by LEED and STM (not shown). This is in line with Lowenstein's rule,[9] which states that Al-O-Al linkages in zeolitic frameworks are forbidden, thus Al/Si = 1 is the largest possible ratio.

One of the most characteristic features of the bilayer silica films is the presence of the two very narrow and intense phonon bands at about 1300 and 690 cm^{-1} in the IRA spectra.[3,4] For the Al-substituted films, no new features are observed in the spectra. As the Al content is increased, the high-frequency peak gradually red-shifts, for example, by about 30 cm^{-1} at $x \approx 0.4$. The intensity and width of this peak are not affected by the incorporation of Al (Supporting Information, Figure S3). Again, this finding is consistent with the fact that the Al atoms do not form any separate phase, but are incorporated into the bilayer structure. The decrease in the phonon frequency can be explained by the inhomogeneity of the otherwise-perfect system of coupled symmetric Si-O-Si oscillators in the pure silica film. In contrast, the low-frequency peak at about 690 cm^{-1} first broadens at $x < 0.2$ and blue-shifts to 702 cm^{-1}, that is, by about 10 cm^{-1} at $x \approx 0.4$.

The above results suggest that Al incorporates into the silica frame by substituting Si in the $[SiO_4]$ tetrahedra. However, there are two non-equivalent sites where Al can substitute Si; that is, in the top and bottom layers (Figure 1 b). Since no extra cations were introduced during the preparation, the charge imbalance caused by the substitution must be compensated either by the metal substrate underneath the film or by protonation of the oxygen atom bridging Si and Al, as is the case for zeolites. As the preparation of the films reported herein involves water-free surroundings, it is plausible that the Al atoms would prefer the bottom layer to be closer to the metal substrate to facilitate the charge transfer. Therefore, it is expected that Al populates the bottom layer first until saturation at $x = 0.25$, and then subsequent Al atoms occupy sites in the top layer. This assumption is supported by the STM results. Indeed, if the distribution of Al atoms within the islands A, shown in Figure 2, follows Lowenstein's rule, then for this film ($x = 0.12$) the islands would cover 0.48 ($= 0.12 \times 4$) of the whole surface, which is in excellent agreement with the 45% coverage observed experimentally.

To form hydroxy groups on the surface, the films were exposed to ca. 400 Langmuirs (1 Langmuir $= 10^{-6}$ Torr sec^{-1}) of H_2O (or D_2O) at about 100 K, which resulted in a solid water overlayer. The film was then heated to 300 K to desorb

weakly bound water molecules. On pure silica films, only small amounts of silanol (Si–OH) groups associated with defect sites were observed by IRAS, showing stretching OH (OD) vibrations $\nu_{O\text{-}H}$ ($\nu_{O\text{-}D}$) at 3750 (2763) cm^{-1}.[10] Upon Al introduction, no other OH related features were detected for the films with an Al content $x < 0.25$. However, at higher Al contents, a peak appears at 3594 cm^{-1}, which falls in the frequency range of the hydroxy groups in the bridging Si-OH_{br}-Al positions in zeolites. For example, in zeolite H-SSZ-13, a high silica form of zeolite chabasite (H-CHA), two different OH_{br} peaks were found at 3616 cm^{-1} and 3584 cm^{-1},[10] which were assigned to the two different oxygen positions of the double six-membered rings, pointing into the supercage and towards the center of the six-membered ring, respectively.[11,12] Therefore, we assigned the 3594 cm^{-1} peak, observed in our films, to Si-OH_{br}-Al species.

The acidity of the Si-OH_{br}-Al groups can be quantified by adsorption of weak bases, such as CO, which binds to the acidic proton through the C atom to form an adduct. This induces a red-shift in $\nu(OH_{br})$, and the magnitude of the shift is proportional to the degree of acidity. As an example, in zeolite H-CHA, one of the most acidic zeolites, the $\nu(OH_{br})$ red-shifts by 316 cm^{-1}. The adsorption is also accompanied by a blue-shift of 38 cm^{-1} in the CO vibration with respect to the free molecule.[10]

Figure 4 shows IRA spectra for an $Al_{0.4}Si_{0.6}O_2$ film exposing OH_{br} (line a) and OD_{br} (line b) groups in a CO ambient (2×10^{-5} mbar) divided by reference spectra taken prior to CO adsorption. Therefore, OH_{br} and OD_{br} absorption signals become positive while negative signals correspond to CO-coordinated OH_{br} (OD_{br}) species. The latter signals are considerably broader and red-shifted by 379 and 243 cm^{-1}, respectively. The CO stretching frequency signal blue-shifts to 2183 cm^{-1}, that is, by 40 cm^{-1} with respect to the gas phase (2143 cm^{-1}), and remains sharp. Therefore, the results clearly show that the acidity of the OH species formed on our aluminosilicate films at high Al/Si ratios is among the highest reported for zeolites.

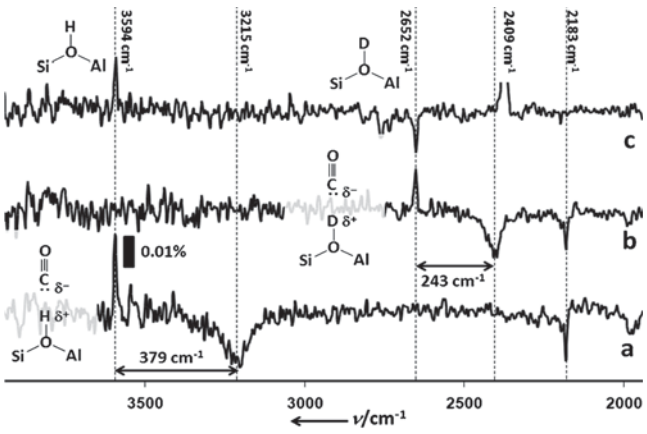

Figure 4. IRA spectra of the $Al_{0.4}Si_{0.6}O_2$ films, hydroxylated with a) H_2O and b) D_2O, recorded in 2×10^{-5} mbar CO atmosphere. The spectra were divided by reference spectra taken before CO exposure. The spectrum (c) is that of the OH-terminated surface upon subsequent hydroxylation with D_2O.

Furthermore, thermal stability experiments showed that the OH_{br} (OD_{br}) group stays on the surface up to a temperature of 650 K. Interestingly, when D_2O is adsorbed on the OH_{br}-containing sample at about 100 K and then the sample is heated to 300 K, the OH_{br} signal at 3594 cm^{-1} disappears (Figure 4c), and the OD_{br} signal appears at 2653 cm^{-1}, thus indicating H/D exchange, which is a well-known phenomenon in zeolite chemistry (see for example Ref. [13]). This finding further corroborates the idea of using these films as suitable model systems for zeolites.

Further support for our interpretation of the experimental results comes from DFT calculations. For a T_8O_{16} unit cell with $AlSi_7O_{16}{\cdot}O_4$/Ru(0001) composition (Figure 1b), the DFT results show that Al prefers the bottom layer, and within the bottom layer it prefers the position above an O atom of the p(2×1)-O/Ru(0001) surface underneath the film. For the hydroxylated film ($HAlSi_7O_{16}{\cdot}O_4$/Ru(0001)), we found that a bridging OH group is most stable one of the two inequivalent positions in the bottom layer, but both form a hydrogen bond to an O atom on the metal surface (OH···O_{surf} bond distances 159 and 144 pm, respectively). This would result in a large red shift and simultaneous broadening of the OH vibrational band, which in turn would render the detection of these sites by IRAS very difficult. In agreement with the experiments, it can be safely concluded that bridging OH groups become visible only if Al starts populating the top layer. For one Al in the top layer, locating the proton at an O1 oxygen atom that bridges the top and bottom layer (Figure 1b) leads to a less stable structure than locating it at one of the two inequivalent oxygen positions within the top layer (O2 and O3). For the latter, OH stretching bands at 3600 and 3598 cm^{-1} were calculated, in excellent agreement with the observed value of 3594 cm^{-1}, whereas the same type of calculations yields 3621 and 3598 cm^{-1} for the O1 and O3 proton positions in H-CHA, respectively; that is, in good agreement with experimentally observed values of 3616 and 3584 cm^{-1}.[10]

Table 1 compares bond distances, angles, and OH and CO stretching frequencies of bridging OH groups in the two-dimensional zeolite-like film on Ru(0001) (H-2D/Ru, for brevity) with those in H-CHA. The Si–O–Al angles, O–H bond distances, and OH stretching frequencies show a monotonous change in the sequence HO3-CHA···H-2D/Ru···HO1-CHA. As the OH bond is longer in H-2D/Ru than in HO1-CHA and is thus weaker, we expect a larger shift of the OH band on CO adsorption, which is indeed found. Both the predicted (349 cm^{-1}) and observed (379 cm^{-1}) shifts of the

Table 1: DFT (PBE + D) results for angles [°], bond distances [pm], and vibrational frequencies [cm^{-1}] of bridging hydroxy groups and their CO adsorption complexes.

	∡SiOAl	r_{OH}	ν_{OH}	ν_{CO}
HO3-CHA	136	97.79	3598	
HO2-2D/Ru	134	97.77	3600	
HO1-CHA	130	97.61	3621	
CO/H-2D/Ru	134	100.42	3252 (−349)	2175 (+43)[a]
CO/HO1-CHA	129	100.06	3299 (−323)	2187 (+55)[a]

[a] gas phase CO: 2132.

OH band for H-2D/Ru are larger than for HO1-CHA. The calculated blue shifts of the CO frequency (43 and 55 cm^{-1}) are also close to the experimentally observed values; that is, 40 cm^{-1} for H-2D/Ru (this work) and 38 cm^{-1} for H-CHA.[10]

In summary, we have presented the preparation of aluminosilicate films weakly bound to a metal support and composed of a bilayer network of $[TO_4]$ (T = Si, Al) tetrahedra forming a sheet of hexagonal prisms with stoichiometry $Al_xSi_{(1-x)}O_2$. At low Al contents ($x < 0.25$), the Al atoms occupy the bottom layer. For $x > 0.25$, Al atoms are present on the top layer, and the O atoms bridging Si and Al atoms can be protonated by water adsorption. The characteristics of the resulting bridging OH_{br} groups perfectly fit into what is known from regular zeolites. They are strongly acidic, as measured by shifts in the OH stretching vibration upon adsorption of CO, and exhibit H–D exchange on D_2O adsorption. These well-defined films constitute the first model system where the surface properties of the inner walls of the pores in zeolites can be modeled by a surface-science approach.

Experimental Section

Experiments were performed in an ultrahigh vacuum system equipped with XPS, LEED, IRAS, and STM. The Ru(0001) surface was cleaned with cycles of Ar^+ sputtering and annealing at 1400 K. The clean surface was pre-covered with a 3O(2×2) overlayer by exposing to 3×10^{-6} mbar O_2 at 1200 K. The films were prepared by sequential Si and Al physical vapor deposition in 2×10^{-7} mbar of O_2. The surface was then oxidized in 3×10^{-6} mbar O_2 at 1200 K for 10 min and slowly cooled down to 450 K in an O_2 environment.

For DFT calculations with periodic boundary conditions, we used the VASP code[14] with the projector augmented wave (PAW) method.[15] As in our previous study of silica films on O-precovered Ru(0001),[3,4] we apply the PBE functional[16] augmented with a semi-empirical $1/r^6$ dispersion term (PBE + D).[17] The cell parameters were fixed to the parameters of the silica double layer on Ru-(0001)(539.6×934.6 pm),[3,4] whereas for chabasite they were optimized for a $(HAlSi_{11}O_{24})_2$ double cell ($a = 942.63$, $b = 937.16$, $c = 1870.8$ pm; $\alpha = 93.5298$, $\beta = 94.1203°$, $\gamma = 94.4907°$). Vibrational frequencies for OH and CO stretching frequencies were calculated from the PBE + D bond distances, making use of the ω/r correlation and anharmonicity corrections proposed by Nachtigall for CO adsorption on zeolite H-ferrierite.[18]

Keywords: density functional calculations · IR spectroscopy · surface structures · thin films · zeolites

[1] C. Martínez, A. Corma, *Coor. Chem. Rev.* **2011**, *255*, 1558 – 1580.
[2] D. Stacchiola, S. Kaya, J. Weissenrieder, H. Kuhlenbeck, S. Shaikhutdinov, H.-J. Freund, M. Sierka, T. K. Todorova, J. Sauer, *Angew. Chem.* **2006**, *118*, 7798 – 7801; *Angew. Chem. Int. Ed.* **2006**, *45*, 7636 – 7639.
[3] D. Löffler, J. J. Uhlrich, M. Baron, B. Yang, X. Yu, L. Lichtenstein, L. Heinke, C. Buchner, M. Heyde, S. Shaikhutdinov, H.-J. Freund, R. Włodarczyk, M. Sierka, J. Sauer, *Phys. Rev. Lett.* **2010**, *105*, 146104.
[4] R. Włodarczyk, M. Sierka, J. Sauer, D. Löffler, J. J. Uhlrich, X. Yu, B. Yang, I. M. N. Groot, S. Shaikhutdinov, H. J. Freund, *Phys. Rev. B* **2012**, *85*, 085403.
[5] L. Lichtenstein, C. Buchner, B. Yang, S. Shaikhutdinov, M. Heyde, M. Sierka, R. Włodarczyk, J. Sauer, H.-J. Freund, *Angew. Chem.* **2012**, *124*, 416 – 420; *Angew. Chem. Int. Ed.* **2012**, *51*, 404 – 407.
[6] B. Yang, X.Yu, J. A. Boscoboinik, L. Lichtenstein, M. Heyde, W. Kaden, R. Włodarczyk, M. Sierka, J. Sauer, S. Shaikhutdinov, H.-J. Freund, in preparation.
[7] E. Dempsey, *J. Catal.* **1974**, *33*, 497.
[8] K.-P. Schroeder, J. Sauer, *J. Phys. Chem.* **1993**, *97*, 6579 – 6581.
[9] W. Lowenstein, *Am. Mineral.* **1954**, *39*, 92.
[10] S. Bordiga, L. Regli, D. Cocina, C. Lamberti, M. Bjørgen, K. P. Lillerud, *J. Phys. Chem. B* **2005**, *109*, 2779 – 2784.
[11] L. J. Smith, A. Davidson, A. K. Cheetham, *Catal. Lett.* **1997**, *49*, 143 – 146.
[12] M. Sierka, J. Sauer, *J. Phys. Chem. B* **2001**, *105*, 1603 – 1613.
[13] C. Tuma, J. Sauer, *Chem. Phys. Lett.* **2004**, *387*, 388 – 394.
[14] G. Kresse, J. Furthmuller, *Phys. Rev. B* **1996**, *54*, 11169 – 11186; *Comput. Mater. Sci.* **1996**, *6*, 15 – 50.
[15] G. Kresse, D. Joubert, *Phys. Rev. B* **1999**, *59*, 1758 – 1775.
[16] J. P. Perdew, K. Burke, M. Ernzerhof, *Phys. Rev. Lett.* **1996**, *77*, 3865 – 3868; J. P. Perdew, K. Burke, M. Ernzerhof, *Phys. Rev. Lett.* **1997**, *78*, 1396.
[17] S. Grimme, *J. Comput. Chem.* **2006**, *27*, 1787 – 1799; T. Kerber, M. Sierka, J. Sauer, *J. Comput. Chem.* **2008**, *29*, 2088 – 2097.
[18] P. Nachtigall, O. Bludsky, L. Grajciar, D. Nachtigallova, M. R. Delgado, C. O. Arean, *Phys. Chem. Chem. Phys.* **2009**, *11*, 791 – 802.